Bioorganic & Medicinal Chemistry xxx (2014) xxx–xxx

Contents lists available at ScienceDirect

Bioorganic & Medicinal Chemistry

journal homepage: www.elsevier.com/locate/bmc

Synthesis and biological comparison of enantiomers of mepenzolate bromide, a muscarinic receptor antagonist with bronchodilatory and anti-inflammatory activities

Yasunobu Yamashita [a], Ken-Ichiro Tanaka [a], Teita Asano [a], Naoki Yamakawa [a], Daisuke kobayashi [a], Tomoaki Ishihara [a], Kengo Hanaya [a], Mitsuru Shoji [a], Takeshi Sugai [a], Mitsuhito Wada [b,c], Tadaaki Mashimo [b,d], Yoshifumi Fukunishi [e], Tohru Mizushima [a,*]

[a] Faculty of Pharmacy, Keio University, Tokyo 105-8512, Japan
[b] Technology Research Association for Next Generation Natural Products Chemistry, 2-3-26, Aomi, Koto-ku, Tokyo 135-0064, Japan
[c] Biochemical Information Project, Fujitsu Limited, 1-9-3, Nakase, Mihama-ku, Chiba 261-8588, Japan
[d] Information and Mathematical Science and Bioinformatics Co., Ltd, Owl Tower, 4-21-1, Higashi-Ikebukuro, Toshima-ku, Tokyo 170-0013, Japan
[e] Molecular Profiling Research Center for Drug Discovery (molprof), National Institute of Advanced Industrial Science and Technology (AIST), Tokyo 135-0064, Japan

ARTICLE INFO

Article history:
Received 5 March 2014
Revised 15 April 2014
Accepted 15 April 2014
Available online xxxx

Keywords:
COPD
Muscarinic receptor
Mepenzolate bromide
Enantiomers

ABSTRACT

Chronic obstructive pulmonary disease (COPD) is characterized by abnormal inflammatory responses and airflow limitations. We recently proposed that the muscarinic antagonist mepenzolate bromide (mepenzolate) would be therapeutically effective against COPD due to its muscarinic receptor-dependent bronchodilatory activity as well as anti-inflammatory properties. Mepenzolate has an asymmetric carbon atom, thus providing us with the opportunity to synthesize both of its enantiomers ((*R*)- and (*S*)-mepenzolate) and to examine their biochemical and pharmacological activities. (*R*)- or (*S*)-mepenzolate was synthesized by condensation of benzilic acid with (*R*)- or (*S*)-alcohol, respectively, followed by quaternization of the tertiary amine. As predicted by computational simulation, a filter-binding assay in vitro revealed that (*R*)-mepenzolate showed a higher affinity for the muscarinic M3 receptor than (*S*)-mepenzolate. In vivo, the bronchodilatory activity of (*R*)-mepenzolate was superior to that of (*S*)-mepenzolate, whereas anti-inflammatory activity was indistinguishable between the two enantiomers. We confirmed that each mepenzolate maintained its original stereochemistry in the lung when administered intratracheally. These results suggest that (*R*)-mepenzolate may have superior properties to (*S*)-mepenzolate as a drug to treat COPD patients given that the former has more potent bronchodilatory activity than the latter.

1. Introduction

Chronic obstructive pulmonary disease (COPD) is currently the fourth leading cause of death in the world and its prevalence and mortality rates are steadily increasing.[1] The most important etiologic factor for COPD is cigarette smoke, with this disease defined by a progressive and not fully reversible airflow limitation associated with abnormal inflammation and emphysema.[1,2] Reactive oxygen species, such as superoxide anion, are believed to play a major role in this abnormal inflammation. Thus, for the clinical treatment of COPD patients, it is important not only to improve the airflow limitation by inducing bronchodilation, but also to suppress disease progression by controlling inflammation via decreased reactive oxygen species.

Bronchodilators (such as muscarinic antagonists) are currently used for the treatment of COPD owing to their ameliorative effect on airflow limitation.[1,2] On the other hand, steroids are used to suppress inflammation in COPD patients; however recent clinical studies revealed that steroids do not significantly modulate disease progression or mortality,[3,4] because the inflammation associated with COPD tends to be resistant to steroid treatment.[5] This insensitivity can be explained in part by the notion that steroids suppress the expression of pro-inflammatory genes via their action on histone deacetylase (HDAC) 2.[6,7] Importantly, it was reported that cigarette smoke inhibits the activity and expression of this protein.[6] Thus, the development of new types of anti-inflammatory drugs to treat COPD patients is highly desirable.

* Corresponding author. Tel.: +81 3 5400 2628.
E-mail address: mizushima-th@pha.keio.ac.jp (T. Mizushima).

http://dx.doi.org/10.1016/j.bmc.2014.04.029
0968-0896/

The number of drugs reaching the marketplace each year is decreasing, mainly due to the unexpected adverse effects of potential drugs being revealed at advanced clinical trial stages. For this reason, we proposed a new strategy for drug discovery and development (drug re-positioning).[8] In this strategy, compounds with therapeutically beneficial activity are screened from a library of approved medicines with a view of developing them for new indications. The advantage of this approach is that there is a decreased risk for unexpected adverse effects in humans because the safety aspects of these drugs have already been well characterized.[8] From a library of approved medicines, we screened compounds that could prevent elastase-induced pulmonary inflammation and emphysema in mice, and selected mepenzolate bromide (mepenzolate).[9] Mepenzolate is an orally administered muscarinic receptor antagonist used to suppress the gastrointestinal hypermotility associated with irritable bowel syndrome.[10–12] We showed that mepenzolate not only exerts an anti-inflammatory effect via a muscarinic receptor-independent mechanism, but also a bronchodilatory effect via a muscarinic receptor-dependent mechanism.[9] This independence of the anti-inflammatory effect is based on observations that other muscarinic receptor antagonists such as ipratropium bromide (ipratropium) and tiotropium bromide (tiotropium) could not exert ameliorative effects against elastase-induced pulmonary emphysema.[9] Although this animal model (elastase-induced pulmonary inflammation and emphysema) does not reflect some of the pathological features of COPD, it has served as a convenient animal model for studying COPD and we reported that mepenzolate could prevent cigarette smoke-induced pulmonary inflammation and emphysema.[9]

As for the mechanism governing the anti-inflammatory activity of mepenzolate, after confirmation of absence of direct inhibitory effect of mepenzolate on elastase, we found that this drug can restore HDAC activity under inflammatory conditions. We also found that mepenzolate, but not steroids, decreased the pulmonary level of superoxide anions. These results may explain why mepenzolate showed superior anti-inflammatory activity compared with steroids in our animal model of COPD.[9,13] Based on these findings, we proposed that mepenzolate could serve as a candidate drug for the treatment of COPD patients, given that it has both anti-inflammatory and bronchodilatory activities. Anti-inflammatory effect of other muscarinic receptor antagonists was also reported recently.[14,15]

Among the five types of muscarinic receptors ($M_{1-5}R$), the muscarinic M3 receptor (M_3R) expressed in airway and intestinal smooth muscle positively regulates bronchoconstriction and intestinal motility, respectively.[16] Mepenzolate is a subtype-non-specific muscarinic antagonist[12] whose bronchodilatory effect and inhibitory effect on intestinal motility can be explained by its antagonistic action on M_3R. On the other hand, the muscarinic M2 receptor (M_2R) expressed in the sinoatrial node of the heart negatively regulates heart rate,[17] and we recently confirmed that mepenzolate's inhibitory action on this receptor leads to an increased heart rate in mice (Tanaka et al., unpublished results).

Mepenzolate has one asymmetric carbon atom (Fig. 1) enabling it to exist in the form of two enantiomers; a racemic mixture ((±)-mepenzolate) of these two enantiomers has been used in a clinical setting. As the synthesis of one or other of these enantiomers of mepenzolate has not been established, it has thus remained unclear which of them is responsible for the drug's anti-inflammatory and anticholinergic activities. In various types of medicines, including drugs used as muscarinic receptor antagonists, differences in stereochemistry can affect the biochemical and pharmacological activities of these compounds, meaning that the isolation of distinct isomers can lead to the clinical development of more effective or safer medicines,[18–20] however, there are still some advantages of racemates (such as cost). In the present study, we have established a protocol for the synthesis of both (*R*)-mepenzolate and (*S*)-mepenzolate (Fig. 1) and examined their biochemical and pharmacological activities. Results showed that although anti-inflammatory activity was indistinguishable between these enantiomers, the binding activity of (*R*)-mepenzolate to human M_3R (hM_3R) in vitro and its bronchodilatory activity in vivo were superior to that of (*S*)-mepenzolate. These findings suggest that (*R*)-mepenzolate may be preferable to (*S*)-mepenzolate as a candidate drug to treat COPD patients.

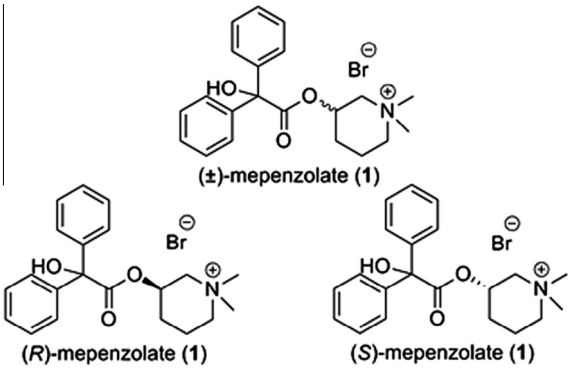

Figure 1. Structures of racemic mepenzolate and its enantiomers.

2. Chemistry

The synthetic route for target compounds is outlined in Scheme 1. The enantiomers of mepenzolate, (*R*)- and (*S*)-mepenzolate ((*R*)-**1** and (*S*)-**1**), were synthesized in two steps from commercially available benzilic acid (**2**) based on a procedure similar to that previously described[21] as outlined in Scheme 1. Condensation of **2** with (*R*)- or (*S*)-3-hydroxy-1-methylpiperidine ((*R*)-**3** or (*S*)-**3**) in the presence of carbonyl diimidazol (CDI) afforded the corresponding enantiomericaly pure tertiary amine ((*R*)- or (*S*)-1-methyl-3-piperidyl benzilate ((*R*)-**4** or (*S*)-**4**)), respectively. Quaternization of intermediate (*R*)-**4** or (*S*)-**4** with methyl bromide in acetonitrile provided desired compound (*R*)-**1** or (*S*)-**1**, respectively.

The final compounds were characterized by nuclear magnetic resonance (NMR), infrared spectroscopy (IR) and high-resolution mass spectra (HR-MS). The enantiomeric purity of each enantiomer of **1** was determined by high performance liquid chromatography (HPLC) with a chiral stationary phase.

3. Results and discussion

3.1. Binding of mepenzolate enantiomers to hM_3R in silico and in vitro

The interaction between hM_3R and (*R*)-mepenzolate (or (*S*)-mepenzolate) was predicted by molecular modelling and docking studies. We constructed the structure of the complex between hM_3R and (*R*)-mepenzolate (or (*S*)-mepenzolate) based on the recent reporting of the crystal structure of the complex between rat M_3R and tiotropium (another muscarinic antagonist[22]) (see Materials and Methods). As for other cases of monoamine receptors,[23] hM_3R has an aspartic acid residue in the third α-helix, identified as $Asp^{3.32}$ (Asp148). This residue of these monoamine receptors strongly interacts with charged nitrogen atoms in the agonists and antagonists,[24] and subsequently we focused on this residue in hM_3R (Asp148).

As shown in Figure 2A, the nitrogen atom (N) in mepenzolate interacts ionically with Asp148; we consider that this interaction

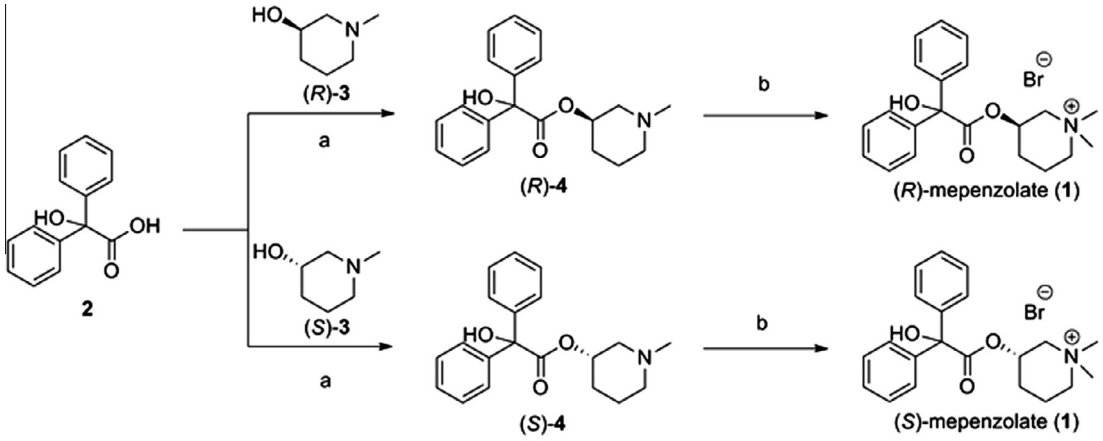

Scheme 1. Synthesis of mepenzolate enantiomers.

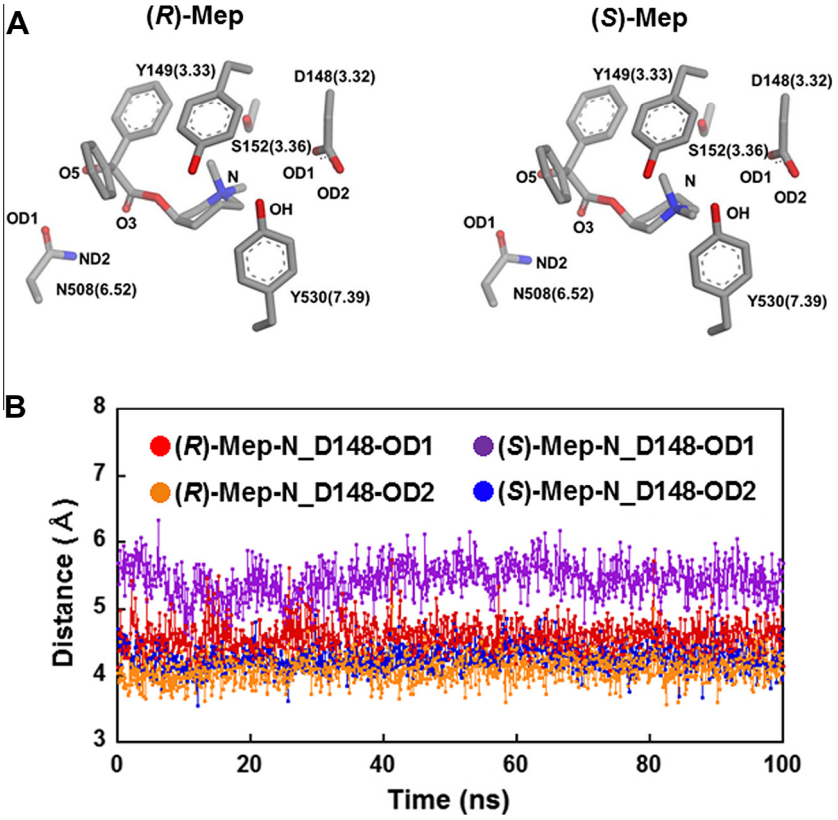

Figure 2. Binding mode of (*R*)-mepenzolate and (*S*)-mepenzolate to hM_3R in silico. (A) Initial coordinates of mepenzolate in hM_3R. Results from MD simulations are shown for (*R*)-mepenzolate ((*R*)-Mep) and (*S*)-mepenzolate ((*S*)-Mep). (B) Interatomic distances between the nitrogen atom (N) of (*R*)-mepenzolate and the two equivalent carboxylate oxygen atoms (OD1 and OD2) of Asp148 of hM_3R during the MD simulation production runs are indicated with red and orange lines, respectively. Those of (*S*)-mepenzolate are indicated with purple and blue lines, respectively.

is important for the association between hM_3R and mepenzolate. We calculated the distance between the nitrogen atom and the two equivalent carboxylate oxygen atoms (OD1 and OD2 in Fig. 2A) of Asp148 during the molecular dynamics (MD) simulation production run. As shown in Figure 2B, the distance was closer for (*R*)-mepenzolate than for (*S*)-mepenzolate (the average distances between OD1 or OD2 of Asp148 and the nitrogen atom of (*R*)-mepenzolate were 4.596 Å or 4.104 Å, respectively, while those for (*S*)-mepenzolate were 5.443 Å or 4.277 Å, respectively). These results suggest that (*R*)-mepenzolate has a higher affinity for hM_3R than (*S*)-mepenzolate.

Other amino acid residues of hM_3R seem to interact with both (*R*)-mepenzolate and (*S*)-mepenzolate in an equivalent manner, as mentioned in the following. $Asn508^{6.52}$ is conserved among all five types of muscarinic receptors and seems to be crucial for ligand recognition.[22,25] Hydrogen bonds between OD1 of $Asn508^{6.52}$ and the hydroxyl oxygen (O5 in Fig. 2A) of (*R*)- or (*S*)-mepenzolate, and between ND2 of $Asn508^{6.52}$ and the carbonyl

oxygen (O3 in Fig. 2A) of (*R*)- or (*S*)-mepenzolate, were stably retained throughout the MD simulations. With regards to these hydrogen bonds, there were no significant differences in the measured distances for the two enantiomers; the average distance between OD1 of Asn508$^{6.52}$ and the hydroxyl oxygen of (*R*)-mepenzolate or (*S*)-mepenzolate was 2.869 Å or 2.846 Å, respectively, while between ND2 of Asn508$^{6.52}$ and the carbonyl oxygen of (*R*)-mepenzolate or (*S*)-mepenzolate the average distance was 2.849 Å or 2.977 Å, respectively. Further to this, no significant differences in the interactions of other residues (Ser152$^{3.36}$, Tyr149$^{3.33}$ and Tyr 530$^{7.39}$) which surround (*R*)- or (*S*)-mepenzolate were found (data not shown). Based on these data, we suggest that the ionic interaction between the charged nitrogen atom and its counter ion Asp148$^{3.32}$ is important for the observed differences in affinity of (*R*)- and (*S*)-mepenzolate for hM_3R.

Our next step was to compare the binding affinities of (*R*)-mepenzolate, (*S*)-mepenzolate and (±)-mepenzolate to hM_3R by carrying out radiolabelled [*N*-methyl-^{3}H]scopolamine methyl bromide ([^{3}H]NMS) displacement studies on this receptor. As shown in Figure 3A, all three forms of mepenzolate inhibit NMS-binding to hM_3R in a dose-dependent manner, showing that they are able to bind to this receptor. The binding affinity of each mepenzolate to hM_3R was compared according to their antagonist dissociation constant K_i value. As shown in Table 1, the K_i value of (*R*)-mepenzolate was less than one-tenth of that of (*S*)-mepenzolate, showing that the former has the much higher affinity for hM_3R than the latter. The K_i value of (±)-mepenzolate was between the values of (*R*)-mepenzolate and (*S*)-mepenzolate (Table 1). We also examined the affinity of each mepenzolate to human M2R (hM2R) using a similar approach. As shown in Figure 3B and Table 1, (*R*)-mepenzolate also exhibited a higher affinity for hM_2R than (*S*)-mepenzolate. Further to this, the data in Table 1 demonstrate that each form of mepenzolate has a higher affinity for hM_2R than for hM_3R.

Table 1
Affinity of (*R*)-mepenzolate, (*S*)-mepenzolate and (±)-mepenzolate for hM_3R and hM_2R

Compound	K_i (nM)	
	hM_2R	hM_3R
(*R*)-Mepenzolate	0.45 ± 0.13	2.11 ± 0.23
(*S*)-Mepenzolate	2.52 ± 0.64	28.0 ± 1.70
(R)-Mepenzolate	0.68 ± 0.01	2.60 ± 0.22

K_i values were calculated based on data shown in Figure 3. Values shown are mean ± SEM (n = 3).

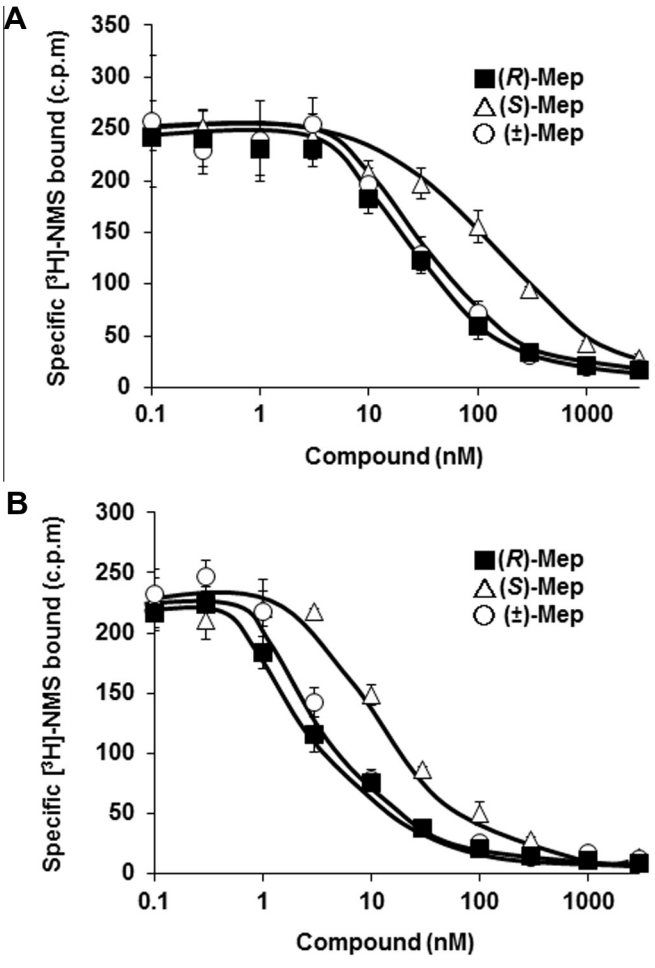

Figure 3. Binding of (*R*)-mepenzolate, (*S*)-mepenzolate and (±)-mepenzolate to hM_3R and hM_2R in vitro. Membrane fractions prepared from cells expressing hM_3R (A) or hM_2R (B) were incubated with radiolabelled NMS (2 nM) in the presence of indicated concentrations of (*R*)-mepenzolate ((*R*)-Mep), (*S*)-mepenzolate ((*S*)-Mep) or (±)-mepenzolate ((±)-Mep) for 2 h and NMS binding was determined by the filter-binding assay. Values shown are mean ± SEM (n = 3).

3.2. Bronchodilatory and anti-inflammatory activities of mepenzolate enantiomers in vivo

We tested for the possibility that enantiomerization of the mepenzolate took place after the administration of (*R*)-mepenzolate or (*S*)-mepenzolate in the lung. Either (*R*)-mepenzolate or (*S*)-mepenzolate was administered intratracheally, and then lung homogenates were prepared and amounts of both enantiomers were assessed by HPLC analysis. As shown in Table 2, (*S*)-mepenzolate or (*R*)-mepenzolate could not be detected after the administration of (*R*)-mepenzolate or (*S*)-mepenzolate, respectively, showing that enantiomerization was not taking place in the lung. The results in Table 2 also show that intratracheally administered mepenzolate rapidly disappears from the lung and that the rate of disappearance is indistinguishable between the two enantiomers.

We then compared the bronchodilatory activities of (*R*)-mepenzolate and (*S*)-mepenzolate based on their capacity to inhibit the increase in airway resistance induced by methacholine.[9] As shown in Figure 4A, at a dose of 38 μg/kg (one twentieth of clinical dose, orally), the intratracheal administration of either (*R*)-mepenzolate or (±)-mepenzolate completely suppressed the methacholine-induced increase in airway resistance; in contrast the suppression by (*S*)-mepenzolate was partial. On the other hand, at a dose of 3.8 μg/kg, (*R*)-mepenzolate and (±)-mepenzolate, but not (*S*)-mepenzolate, showed an inhibitory effect on the methacholine-induced increase in airway resistance (Fig. 4B). These results show that (*R*)-mepenzolate has a more potent bronchodilatory activity than (*S*)-mepenzolate. Considering that the bronchodilatory activity of mepenzolate is mediated via its antagonistic activity on M_3R, and the fact that the M_3R amino acid sequence homology between human and mouse is relatively high (97.4%), the results in Figure 4 are consistent with those shown in Figure 3.

We next compared the anti-inflammatory activities of (*R*)-mepenzolate and (*S*)-mepenzolate. Porcine pancreatic elastase (PPE)-induced pulmonary inflammatory responses were monitored as a function of the number of leucocytes in bronchoalveolar lavage fluid (BALF). As shown in Figure 5A, the total number of leucocytes and the individual number of neutrophils in BALF increased after the PPE treatment; this increase was partially suppressed by the simultaneous intratracheal administration of each mepenzolate. The extent of suppression was indistinguishable between (*R*)-mepenzolate, (*S*)-mepenzolate and (±)-mepenzolate at doses of 7.5 and 38 μg/kg (Fig. 5A). We also monitored

Table 2
Pulmonary levels of (*R*)-mepenzolate and (*S*)-mepenzolate after intratracheal administration of (*R*)-mepenzolate or (*S*)-mepenzolate. Mice were intratracheally administered (*R*)-mepenzolate or (*S*)-mepenzolate (20 mg/kg), and lung homogenates were prepared after indicated periods

Compound	Tissue concentration (μg/lung)					
	(*R*)-mepenzolate			(*S*)-mepenzolate		
	5 min	15 min	30 min	5 min	15 min	30 min
(*R*)-Mepenzolate	44.5 ± 11.5	6.3 ± 4.2	5.1 ± 1.3	n.d.	n.d.	n.d.
(*S*)-Mepenzolate	n.d.	n.d.	n.d.	36.4 ± 9.5	7.6 ± 0.5	6.2 ± 0.4

Levels of (*R*)-mepenzolate and (*S*)-mepenzolate were determined as described in the Materials and Methods. Values are mean ± SEM ($n = 3$). n.d., not detected.

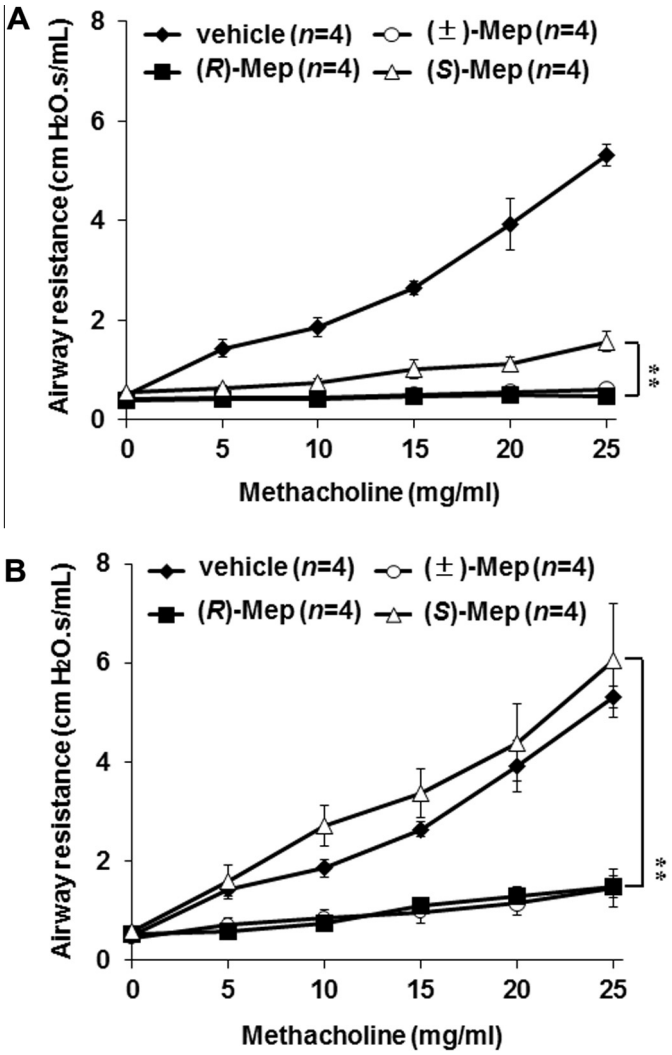

Figure 4. Effect of intratracheal administration of (*R*)-mepenzolate, (*S*)-mepenzolate and (±)-mepenzolate on methacholine-induced airway constriction. (*R*)-mepenzolate ((*R*)-Mep), (*S*)-mepenzolate ((*S*)-Mep) or (±)-mepenzolate ((±)-Mep) at 38 (A) or 3.8 (B) μg/kg was administered intratracheally. After 1 h, mice were exposed to nebulized methacholine 5 times for 20 s with a 40 s interval between exposures and airway resistance was determined after each methacholine challenge as described in the Experimental section. Values shown are mean ± SEM. $^{**}P < 0.01$ ((*R*)-mepenzolate versus (*S*)-mepenzolate).

PPE-induced pulmonary inflammatory responses based on the levels of pro-inflammatory cytokines (tumor necrosis factor (TNF)-α) and chemokines (macrophage inflammatory protein (MIP)-2, monocyte chemotactic protein (MCP)-1 and keratinocyte-derived chemokine (KC)) in BALF. These levels were increased by the PPE administration, with this increase partially suppressed by the simultaneous intratracheal administration of either (*R*)-mepenzolate, (*S*)-mepenzolate or (±)-mepenzolate, with the extent of suppression indistinguishable between the three forms (Fig. 5B). The results in Figure 5 suggest that the anti-inflammatory effect afforded by (*R*)-mepenzolate and (*S*)-mepenzolate is indistinguishable. Although the primary target molecule mediating the anti-inflammatory activity of mepenzolate is not known as yet, it would seem that, in contrast to the case of M_3R, both enantiomers have similar affinity or intrinsic efficacy for this target molecule.

3.3. Adverse effects of mepenzolate enantiomers in vivo

In relation to the clinical application of mepenzolate to treat COPD patients, constipation and arrhythmia (heart palpitations) have been noted as adverse side effects of this drug as a consequence of its inhibitory effect on muscarinic receptors.[26,27] To this end, we compared the effects of (*R*)-mepenzolate and (*S*)-mepenzolate on defecation and heart rates in mice. Since the efficiency of absorption of intratracheally administered mepenzolate into the circulation is low (Tanaka et al., unpublished results), much higher dose of mepenzolate was predicted to be required to affect defecation and heart rates, compared to bronchodilatory and anti-inflammatory activities.

Mice were subjected to restraint stress as a means to increase fecal pellet output. As shown in Figure 6, the administration of either (*R*)-mepenzolate or (±)-mepenzolate (4.7 mg/kg) suppressed fecal pellet output with respect to control (vehicle) mice. (*S*)-mepenzolate (4.7 mg/kg) also showed a tendency to suppress fecal pellet output, but the suppression was not statistically significant (Fig. 6). These findings suggest that (*R*)-mepenzolate has a more potent inhibitory effect on fecal pellet output than (*S*)-mepenzolate. Since M_3R expressed in the intestinal smooth muscle regulate intestinal motility, the results in Figure 6 can be explained in terms of the higher relative affinity for M_3R of (*R*)-mepenzolate than (*S*)-mepenzolate (Fig. 3A and Table 1).

The effect of mepenzolate on heart rate was measured by infrared sensor. As shown in Figure 7, the separate administration of (*R*)-mepenzolate, (*S*)-mepenzolate and (±)-mepenzolate increased heart rate to a similar extent. Since the stimulation of M_2R expressed in the heart mediates a reduction of heart rate, the results in Figure 7 are not consistent with (*R*)-mepenzolate having a higher relative affinity for M_2R than (*S*)-mepenzolate (Fig. 3B and Table 1). This contradiction may be explained by differences in the sensitivities of the assays used, where the in vitro filter-binding assay is more sensitive than the in vivo heart rate assay. Furthermore, the difference in binding affinity between (*R*)-mepenzolate and (*S*)-mepenzolate is larger for M_3R than for M_2R (Fig. 3 and Table 1), which may explain why the difference between (*R*)-mepenzolate and (*S*)-mepenzolate for fecal pellet output is clearer than that for heart rate.

Since COPD is characterized by airflow limitation and abnormal inflammatory responses, a combination of anti-inflammatory drugs (such as steroids) and bronchodilators is the standard treatment regime.[28,29] Since mepenzolate has both anti-inflammatory and bronchodilatory activities, this drug may be beneficial for treating COPD without the concomitant use of other medications. In this study, we compared the bronchodilatory and anti-inflam-

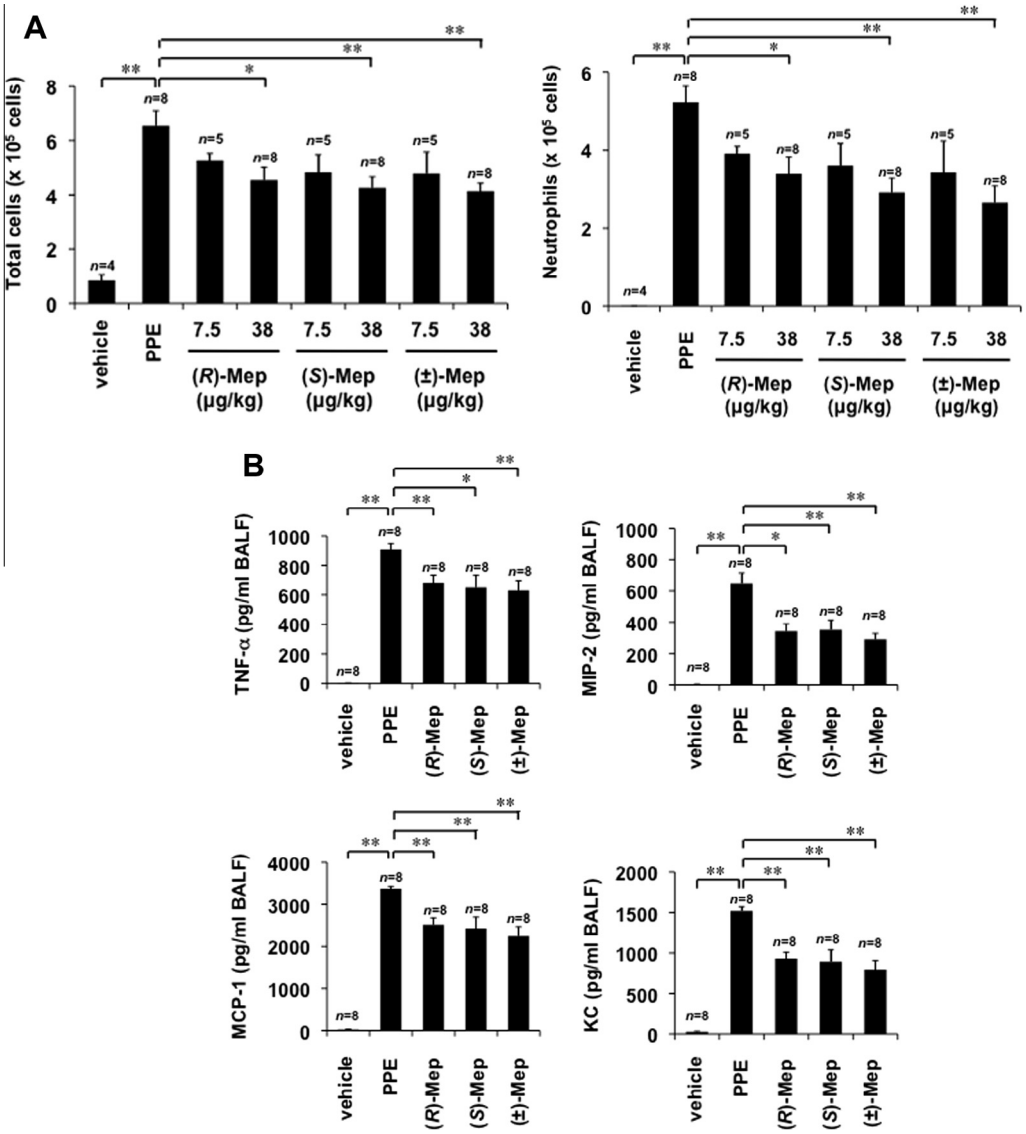

Figure 5. Effect of intratracheal administration of (*R*)-mepenzolate, (*S*)-mepenzolate and (±)-mepenzolate on PPE-induced pulmonary inflammatory responses. The indicated dose of 7.5 or 38 μg/kg of (*R*)-mepenzolate ((*R*)-Mep), (*S*)-mepenzolate ((*S*)-Mep) or (±)-mepenzolate ((±)-Mep) was administered intratracheally, and 1 h later mice were treated with or without (vehicle) PPE (20 U/kg). Six hours after the PPE administration, BALF was prepared. The total cell number and the number of neutrophils were determined as described in the Experimental section (A). The amounts of TNF-α, MIP-2, MCP-1 and KC in BALF were determined by ELISA (B). Values shown are mean ± SEM. $^{*}P$ <0.05; $^{**}P$ <0.01.

matory activities of (*R*)-mepenzolate and (*S*)-mepenzolate and found that although the anti-inflammatory activity was indistinguishable between the two enantiomers, the bronchodilatory activity of (*R*)-mepenzolate was superior to that of (*S*)-mepenzolate. These results suggest that (*R*)-mepenzolate is likely to be more appropriate than (*S*)-mepenzolate as a drug to treat COPD patients. However, we also found that (*R*)-mepenzolate has a more potent inhibitory effect on fecal pellet output than (*S*)-mepenzolate, suggesting that (*R*)-mepenzolate may cause more severe constipation than (*S*)-mepenzolate as an adverse side effect associated with its use. However, it should be noted that the intratracheally administered mepenzolate showed both anti-inflammatory and bronchodilatory effects in mice at a much lower dose than that which affected defecation and heart rates. For this reason we consider that intratracheally administered mepenzolate may achieve both its anti-inflammatory and bronchodilatory effects without affecting intestinal motility and heart rate in a clinical setting.

The relationship between the stereochemistry and potency of activity for various muscarinic receptor antagonists has been studied, and it was suggested that the former greatly affects the latter.[30,31] In particular, similar to mepenzolate, 3-quinuclidinyl benzilate has an asymmetric carbon at the C3 position of the piperidine skeleton containing a tertiary amine; it was reported that (*R*)-3-quinuclidinyl benzilate has a higher affinity for muscarinic receptors than (*S*)-3-quinuclidinyl benzilate.[30] Furthermore, aclidinium bromide and glycopyrronium bromide (glycopyrronium), both of which are muscarinic receptor antagonists and used clinically for COPD patients, also have an asymmetric carbon at this position and it was suggested that the (*R*)-isomer of each of these has a higher affinity for M_3R than the corresponding (*S*)-isomer.[32] Thus, it is interesting that mepenzolate shares similar stereochemistry and pharmacological properties with these other M_3R antagonists.

It is difficult to determine which of (*R*)-mepenzolate and (±)-mepenzolate should be developed as a drug to treat COPD patients, as anti-inflammatory activity, bronchodilatory activity, inhibitory effect on fecal pellet output, and stimulatory effect on heart rate were indistinguishable between the two forms. Because (*R*)-mepenzolate has a higher affinity for hM_3R than (*S*)-mepenzolate, (*R*)-mepenzo-

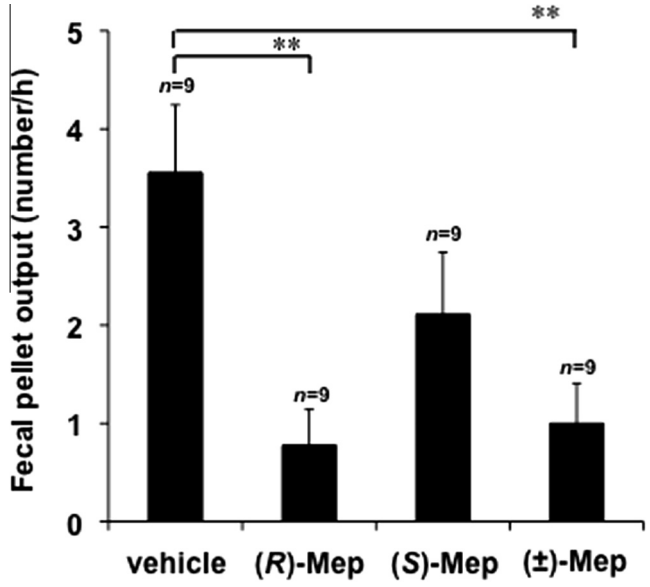

Figure 6. Effect of intratracheal administration of (*R*)-mepenzolate, (*S*)-mepenzolate and (±)-mepenzolate on fecal pellet output. (*R*)-mepenzolate ((*R*)-Mep), (*S*)-mepenzolate ((*S*)-Mep) or (±)-mepenzolate ((±)-Mep) (4.7 mg/kg) was administered intratracheally and one hour later mice were exposed to restraint stress. The number of fecal pellets excreted during the restraint stress period (1 h) was determined. Values shown are mean ± SEM. $^{**}P$ <0.01.

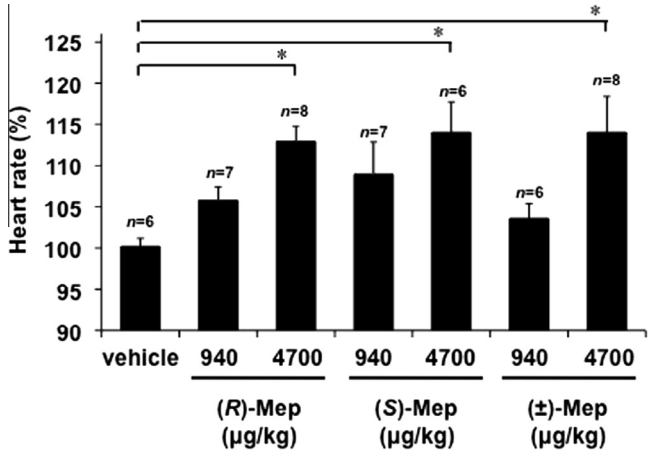

Figure 7. Effect of intratracheal administration of (*R*)-mepenzolate, (*S*)-mepenzolate and (±)-mepenzolate on heart rate. The indicated doses of (*R*)-mepenzolate ((*R*)-Mep), (*S*)-mepenzolate ((*S*)-Mep) or (±)-mepenzolate ((±)-Mep) were administered intratracheally. The alteration of heart rate (beats per minute) was monitored as described in the Experimental section, with the mepenzolate-dependent alteration of heart rate (percentage change from the baseline to peak) calculated. Values shown are mean ± SEM. $^{*}P$ <0.05.

late may be more effective and safer for clinical use than (±)-mepenzolate. On the other hand, a significant advantage of (±)-mepenzolate is that it already has regulatory approval, and some pre-clinical tests (such as genotoxicity tests) could be omitted from the battery of tests required for the approval. Therefore, it would perhaps be better to initially consider (±)-mepenzolate for the treatment of COPD, followed by the development and subsequent introduction of (*R*)-mepenzolate.

Muscarinic antagonists used for COPD are usually categorised as being long-acting (such as tiotropium and glycopyrronium) or short-acting (such as ipratropium) and we previously reported that mepenzolate belongs to short-acting ones.[9] Furthermore, the clinical dose of tiotropium (18 μg/day) or glycopyrronium (50 μg/day) for COPD is much lower than that of ipratropium (160 μg/day) and we previously reported that the dose–response profile of mepenzolate for bronchodilation was similar to that of ipratropium.[9] These results suggest that mepenzolate may be inferior to tiotropium and glycopyrronium as a bronchodilator. On the other hand, we recently reported that steroids do not provide protective or therapeutic benefits against PPE-induced pulmonary emphysema, alterations of lung mechanics or respiratory dysfunction,[33] whereas we showed that mepenzolate is effective against these disorders under the same experimental conditions.[9] Furthermore, we reported that glycopyrronium suppressed the PPE-induced pulmonary emphysema and alterations of lung mechanics, however, the extent of suppression of emphysema was not as apparent as that seen with mepenzolate, and glycopyrronium did not significantly suppress the PPE-induced respiratory dysfunction.[9] Tiotropium did not suppress the PPE-induced pulmonary emphysema, alterations of lung mechanics, or respiratory dysfunction.[9] These results suggest that mepenzolate may be superior to steroids, tiotropium and glycopyrronium as an anti-inflammatory drug. Thus, we consider that chemical modification of (*R*)-mepenzolate, which is aimed both to change its bronchodilatory effect from short-acting to long-acting and to maintain its anti-inflammatory activity, would be important for identification more therapeutically beneficial drugs for COPD.

4. Conclusion

Results in this study suggest that (*R*)-mepenzolate may have superior properties to (*S*)-mepenzolate as a drug to treat COPD patients given that the former has more potent bronchodilatory activity than the latter.

5. Experimental section

5.1. Chemicals and animals

All organic solvents and reagents used for the synthesis were purchased from commercial sources and used without further purification. (*R*)- and (*S*)-3-hydroxy-1-methylpiperidine were from Pharma Block (Nanjing, China). Mepenzolate, PPE and HPLC-grade acetonitrile were obtained from Sigma–Aldrich (St. Louis, MO). Novo-Heparin for injection was from Mochida Pharmaceutical Co. (Tokyo, Japan). Chloral hydrate was from Nacalai Tesque (Kyoto, Japan). Diff-Quik was from Sysmex Co (Kobe, Japan). Isoflurane was from Pfizer (New York, NY). The Amicon ultra-0.5 centrifugal filter that we used was purchased from Merck Millipore (Billerica, MA). ELISA kits for TNF-α, MIP-2, MCP-1 and KC were from R&D Systems (Minneapolis, MN). Other solvents and reagents were purchased from Tokyo Chemical Industry Co., Ltd (Tokyo, Japan) or Wako Pure Chemical Industries (Tokyo, Japan). ICR mice (4–6 weeks old, male) were purchased from Charles River (Yokohama, Japan). The experiments and procedures described here were carried out in accordance with the Guide for the Care and Use of Laboratory Animals as adopted and promulgated by the National Institutes of Health, and were approved by the Animal Care Committee of Keio University.

5.2. Chemistry

Fourier transform IR spectra were recorded on a Jeol FT-IR SPX60 spectrometer as attenuated total reflection for a solid. ^{1}H NMR and ^{13}C NMR spectra were recorded on a VARIAN 500-MR spectrometer (Agilent Technologies Japan, Tokyo, Japan) operating at 500 MHz, in a ca. 2% solution of dimethyl sulfoxide (DMSO)-d_6. Coupling constant (J) values below are estimated in hertz (Hz) and spin multiples are given as s (singlet), d (doublet), and m (mul-

tiplet). HR-MS were measured on a Jeol JMS-700 MStation. The progress of all reactions was monitored by thin-layer chromatography with silica gel glass plates (60 F_{254}) (Merck Ltd, Tokyo, Japan), and spots were visualized with ultraviolet light (254 nm) and stained with 5% ethanolic phosphomolybdic acid. Column chromatography was performed using silica gel 60N (Kanto Chemical Co., Tokyo, Japan).

HPLC-UV chromatograms were acquired in a Waters Alliance 2695 chromatographer equipped with a Waters 2996 photodiode array detector (Waters, Milford, MA). HPLC analysis was conduced according to method A (see below) with the retention time expressed in min detected at 220 nm. For HPLC method A, chromatography was performed on a Daicel Chiralpak IA (250 mm × 46 mm). The mobile phase, at a flow of 1.0 mL/min, was a binary gradient of water (containing 0.1 M potassium hexafluorophosphate) and acetonitrile, 30:70.

5.2.1. (*R*)-Mepenzolate ((*R*)-1)

To a solution of benzilic acid (830 mg, 3.6 mmol) in *N*,*N*-dimethylformamide (DMF) (8 mL), CDI (883 mg, 5.4 mmol) was added and the mixture was stirred for 15 min at room temperature. To this mixture, a solution of (*R*)-**3** (500 μL, 4.3 mmol) in DMF (4 mL) was added dropwise at 80 °C and the resulting mixture was stirred for 18 h at the same temperature. After cooling to room temperature, the reaction was quenched with water and organic materials were extracted with ethyl acetate. The combined extract was washed with brine, dried over sodium sulfate and concentrated in vacuo. The residue was then applied to a short silica gel column, eluted with ethyl acetate and concentrated in vacuo to give (*R*)-**4** as a yellow oil, which was used for the next step without further purification.

To a solution of (*R*)-**4** (860 mg, 2.6 mmol) in acetonitrile (10 mL), methyl bromide (2.0 M in tetrahydrofuran, 6.2 mL, 12.4 mmol) was added and stirred for 5 h at room temperature. The precipitates were filtered off and re-crystallized from dichloromethane and methanol to give (*R*)-**1** as colorless fine needles (980 mg, 64% 2 steps). IR ν_{max}: 3432, 3315, 1735, 1216, 1093, 1068, 923, 705 cm^{-1}; ^1H NMR (DMSO-d_6): δ = 7.28–7.37 (m, 10H), 6.82 (s, 1H), 5.28 (m, 1H), 3.63 (dd, *J* = 13.5, 3.5 Hz, 1H), 3.49 (dd, *J* = 13.5, 4.7 Hz, 1H), 3.37 (m, 1H), 3.33 (m, 1H), 3.10 (s, 3H), 2.82 (s, 3H), 1.63–1.85 (m, 4H); ^{13}C NMR (DMSO-d_6): δ = 171.9, 143.0, 142.7, 128.0, 127.9, 127.7, 127.6, 127.0, 80.7, 66.8, 61.6, 60.8, 25.2, 16.2; $[\alpha]_D^{26}$ −8.12 (*c* 1.00, methanol); mp 224.2–224.9 °C; HR-MS (FAB): calcd for $C_{21}H_{26}O_3N$: $[M+1]^+$: 340.1913; found: *m*/*z* = 340.1905. HPLC analysis was done according to method A (retention time, 16.8 min; single peak).

5.2.2. (*S*)-Mepenzolate ((*S*)-1)

The title compound ((*S*)-**1**) was synthesized using the same procedure described for the preparation of (*R*)-mepenzolate, except for the use of (*S*)-3-hydroxy-1-methylpiperidine instead of (*R*)-isomer. The final sample was a colorless needle (934 mg, 61% 2 steps). $[\alpha]_D^{25}$ +8.33 (*c* 1.00, methanol). Other physical and spectral data of this enantiomer were in good accordance with those of (*R*)-**1**. HPLC analysis was done according to method A (retention time, 15.0 min; single peak).

5.3. Filter-binding assay

The filter-binding assay was done as described previously[34] with some modifications. Membrane fractions prepared from CHO-K1 cells expressing hM2R or hM_3R (Membrane Target Systems, Perkin–Elmer Life and Analytical Sciences, Boston, MA; protein concentration, 10 μg/well) were incubated with 2 nM $[^3H]$NMS (85.5 Ci/mmol) at room temperature for 2 h in 200 μL PBS in the presence of each mepenzolate. A range of concentrations (10^{-10} to 3×10^{-5} M) of each mepenzolate were tested in triplicate to generate competition curves. Non-specific binding was determined in the presence of atropine (2.5 μM). The samples were passed through a GF/C filter (Filtermat A, PerkinElmer Life and Analytical Sciences, Boston, MA) that was pre-incubated for 1 h with wash buffer (50 mM Tris/HCl (pH 7.4), 100 mM NaCl) containing 1.0% polyethylenimine, and washed four times with ice-cold wash buffer. Filters were then dried for 30 min before attachment to MeltiLex A (melt-on scintillation sheet; PerkinElmer Life and Analytical Sciences, Boston, MA). The radioactivity remaining on the filter was monitored with MicroBeta Trilux microplate scintillation counter (PerkinElmer Life and Analytical Sciences, Boston, MA). Affinities at equilibrium were determined as equilibrium antagonist dissociation constant (K_i) values after correcting the experimentally determined IC_{50} values with the experimentally determined K_d value of NMS for hM_2R or hM_3R and the concentration of NMS, as described previously.[35] The K_i value was obtained from three independent curves. All adjustments were performed using Prism (GraphPad Software, Inc., San Diego, CA).

5.4. Homology modelling

The structure of rat M_3R bound to its antagonist, tiotropium, was recently solved by X-ray crystallography (PDB code 4DAJ.[22] Although a T4-lysozyme was fused to intracellular loop 3 (ICL3) for enhancing crystallization, there were no residue gaps and few residue mismatches between the crystal structure and hM_3R amino acid sequence except for both terminus regions and the ICL3. Therefore, we constructed an hM_3R model by fixing the missing atoms in the crystal and replacing the mismatched amino acid residues with human ones. The fused T4-lysozyme is replaced with a ten amino acid linker sequence (GGGGSGGGGS), because this region has no reliable template for modelling. These modelling procedures were performed using Modeller v9.4.[36]

5.5. Molecular dynamics

MD simulations were carried out in an explicit membrane and water system by using myPresto/cosgene.[37] The whole structure consists of the hM_3R model, (*R*)-**1** or (*S*)-**1**, four cholesterols, 146 1-palmitoyl-2-oleoyl-sn-glycero-3-phosphocholine and 10,212 water molecules (TIP3P model) including 21 Na^+ and 35 Cl^- particles.[38] NaCl was added to achieve the saline condition and excessive Cl^- was added to neutralize the total charge of the system. The AMBER99 force field parameters[39] were used for hM_3R. Force field parameters for (*R*)- or (*S*)-mepenzolate were obtained according to the generalized AMBER force field procedure[40] with partial charges derived from quantum chemical calculations by GAUSSIAN 03 at the HF/6-31G* level of theory. Periodic boundary conditions were applied and Berendsen's method for temperature and pressure coupling was adopted (300 K and 1 atm, respectively). After performing 400 steps of energy minimization by the steepest descent method and the conjugate gradient method, the NPT (constant particle number, constant pressure, and constant temperature)[41] for 200 ps was performed to obtain an equilibrated system with the following conditions: periodic boundary, 300 K, 1 atm, cutoff = 12 Å, and 1.0 fs/step. The ZD method[42] (α = 0.0 $Å^{-1}$) was applied for the calculation of electrostatic force terms. Further 200 ps equilibrium calculations were performed under NVT (constant particle number, constant volume, and constant temperature) conditions with the cell size maintained (300 K, 1.0 fs/step for 50 ps, 0.75 fs/step for 60 ps, 1.0 fs/step for 40 ps and 2.0 fs/step for 50 ps). After these preliminary calculations, a production run at 300 K was performed with the same cell size and the time step was set to 2 fs. The SHAKE algorithm was applied to fix all the bonds involving hydrogen during the NVT simulations. Snapshot

structures were obtained at every 10 ps as the target structure was extracted from a trajectory of 100 ns.

5.6. Treatment of mice with PPE and mepenzolate

Mice maintained under anaesthesia with isoflurane were intratracheally administered PPE (20 U/kg) or each mepenzolate (various doses) in sterile saline (1 ml/kg) via micropipette. For control mice, sterile saline alone was administered by the same procedure. The administration of mepenzolate was performed 1 h prior to the PPE administration.

5.7. Measurement of airway resistance

Airway resistance was monitored with a computer-controlled small-animal ventilator (FlexiVent, SCIREQ, Montreal, Canada), as described previously.[13] Mice were anesthetized with chloral hydrate (500 mg/kg), after 20 min a tracheotomy was performed, and an 8 mm-long section of metallic tube (outer or inner diameter, 1.27 mm or 0.84 mm, respectively) was inserted into the trachea. Mice were mechanically ventilated at a rate of 150 breaths/min, using a tidal volume of 8.7 ml/kg and a positive end-expiratory pressure of 2–3 cmH_2O. For measurement of methacholine-induced increases in airway resistance, 1 h after the mepenzolate administration, mice were exposed to nebulised methacholine (5 mg/ml) five times for 20 s with a 40 s interval between exposures, and airway resistance was measured after each methacholine challenge by the snapshot technique. All data were analysed using FlexiVent software.

5.8. Analysis of PPE-induced inflammatory responses

Six hours after the PPE administration, BALF was collected by cannulating the trachea and lavaging the lung with 1 ml of sterile saline containing 50 U/ml heparin (2 times). About 1.8 ml of BALF was routinely recovered from each animal. The total cell number was counted using a hemocytometer. Cells were stained with Diff-Quik reagents after centrifugation with Cytospin® 4 (Thermo Electron Corporation, Waltham, MA), and the ratio of number of neutrophils to total cell number was calculated. Cytokine and chemokine levels were measured by ELISA, according to the manufacturer's protocol.

5.9. Analysis of fecal pellet output

One hour after the mepenzolate administration, mice were subjected to restraint stress by being placed individually into a 50 ml tube (Becton Dickinson, Franklin Lakes, NJ) for 1 h, as described previously.[43] These tubes are small enough to restrain a mouse so that it is able to breathe but unable to move freely. The number of fecal pellets excreted during the restraint stress period (1 h) was measured.

5.10. Measurement of heart rate

Heart rate was measured with a MouseOx system (STARR Life Sciences Corp., Allison Park, PA), as described previously.[44] Mice were anesthetized with chloral hydrate (500 mg/kg) and after 20 min the sensor was attached to the thigh. Heart rate was determined immediately after the mepenzolate administration, using MouseOx software (STARR Life Sciences Corp., Allison Park, PA).

5.11. Determination of the level of mepenzolate in the lung

Whole lungs were taken from mepenzolate-treated mice, homogenised in sterile PBS containing 50 U/ml heparin, and centrifuged to obtain the final sample. An aliquot (300 μl) of each sample was ultrafiltered with an Amicon ultra-0.5 centrifugal filter to extract the mepenzolate. The filtrate was analysed by analytical HPLC using method A (see above).

5.12. Statistical analysis

All values are expressed as the mean ± SEM Tukey's test was used to evaluate differences between three or more groups. Differences were considered to be significant for values of $P < 0.05$.

Acknowledgments

This work was supported by Grants-in-Aid of Scientific Research from the Ministry of Health, Labour, and Welfare of Japan, Grants-in-Aid for Scientific Research from the Ministry of Education, Culture, Sports, Science and Technology of Japan, and Grants-in-Aid of the Japan Science and Technology Agency.

Supplementary data

Supplementary data (^1H NMR and ^{13}C NMR spectra of final compounds for (*R*)-mepenzolate (**1**) and (*S*)-mepenzolate (**1**)) associated with this article can be found, in the online version, at http://dx.doi.org/10.1016/j.bmc.2014.04.029.

References and notes

1. Rabe, K. F.; Hurd, S.; Anzueto, A.; Barnes, P. J.; Buist, S. A.; Calverley, P.; Fukuchi, Y.; Jenkins, C.; Rodriguez-Roisin, R.; van Weel, C.; Zielinski, J. *Am. J. Respir. Crit. Care Med.* **2007**, *176*, 532.
2. Barnes, P. J.; Stockley, R. A. *Eur. Respir. J.* **2005**, *25*, 1084.
3. Alsaeedi, A.; Sin, D. D.; McAlister, F. A. *Am. J. Med.* **2002**, *113*, 59.
4. Calverley, P. M.; Anderson, J. A.; Celli, B.; Ferguson, G. T.; Jenkins, C.; Jones, P. W.; Yates, J. C.; Vestbo, J. *N. Engl. J. Med.* **2007**, *356*, 775.
5. Barnes, P. J.; Ito, K.; Adcock, I. M. *Lancet* **2004**, *363*, 731.
6. Rajendrasozhan, S.; Yang, S. R.; Edirisinghe, I.; Yao, H.; Adenuga, D.; Rahman, I. *Antioxid. Redox Signal.* **2008**, *10*, 799.
7. Ito, K.; Yamamura, S.; Essilfie-Quaye, S.; Cosio, B.; Ito, M.; Barnes, P. J.; Adcock, I. M. *J. Exp. Med.* **2006**, *203*, 7.
8. Mizushima, T. *J. Biochem.* **2011**, *149*, 499.
9. Tanaka, K.; Ishihara, T.; Sugizaki, T.; Kobayashi, D.; Yamashita, Y.; Tahara, K.; Yamakawa, N.; Iijima, K.; Mogushi, K.; Tanaka, H.; Sato, K.; Suzuki, H.; Mizushima, T. *Nat. Commun.* **2013**, *4*, 1.
10. Chen, J. Y. *Arch. Int. Pharmacodyn. Ther.* **1959**, *121*, 78.
11. Buckley, J. P.; De, F. J.; Reif, E. C. *J. Am. Pharm. Assoc. Am. Pharm. Assoc. (Baltim)* **1957**, *46*, 592.
12. Long, J. P.; Keasling, H. H. *J. Am. Pharm. Assoc. Am. Pharm. Assoc. (Baltim)* **1954**, *43*, 616.
13. Tanaka, K.; Sato, K.; Aoshiba, K.; Azuma, A.; Mizushima, T. *Am. J. Physiol. Lung Cell. Mol. Physiol.* **2012**, *302*, L1250.
14. Bosnjak, B.; Tilp, C.; Tomsic, C.; Dekan, G.; Pieper, M. P.; Erb, K. J.; Epstein, M. M. *Pulm. Pharmacol. Ther.* **2014**, *27*, 44.
15. Shen, L. L.; Liu, Y. N.; Shen, H. J.; Wen, C.; Jia, Y. L.; Dong, X. W.; Jin, F.; Chen, X. P.; Sun, Y.; Xie, Q. M. *Int. Immunopharmacol.* **2014**, *18*, 358.
16. Eglen, R. M.; Hegde, S. S.; Watson, N. *Pharmacol. Rev.* **1996**, *48*, 531.
17. Eglen, R. M. *Prog. Med. Chem.* **2005**, *43*, 105.
18. Richter, J. E.; Kahrilas, P. J.; Johanson, J.; Maton, P.; Breiter, J. R.; Hwang, C.; Marino, V.; Hamelin, B.; Levine, J. G. *Am. J. Gastroenterol.* **2001**, *96*, 656.
19. Bauernfeind, A. *J. Antimicrob. Chemother.* **1999**, *43*, 77.
20. Bartlett, J. B.; Dredge, K.; Dalgleish, A. G. *Nat. Rev. Cancer* **2004**, *4*, 314.
21. Dolle, F.; Hinnen, F.; Vaufrey, F.; Demphel, S.; Bramoulle, Y.; Fournier, D.; Ponchant, M.; Valette, H.; Crouzel, C. *J. Labelled Compd. Rad.* **2001**, *44*, 337.
22. Kruse, A. C.; Hu, J.; Pan, A. C.; Arlow, D. H.; Rosenbaum, D. M.; Rosemond, E.; Green, H. F.; Liu, T.; Chae, P. S.; Dror, R. O.; Shaw, D. E.; Weis, W. I.; Wess, J.; Kobilka, B. K. *Nature* **2012**, *482*, 552.
23. Venkatakrishnan, A. J.; Deupi, X.; Lebon, G.; Tate, C. G.; Schertler, G. F.; Babu, M. M. *Nature* **2013**, *494*, 185.
24. Suga, H.; Ehlert, F. J. *Biochemistry* **2013**, *52*, 4914.
25. Haga, K.; Kruse, A. C.; Asada, H.; Yurugi-Kobayashi, T.; Shiroishi, M.; Zhang, C.; Weis, W. I.; Okada, T.; Kobilka, B. K.; Haga, T.; Kobayashi, T. *Nature* **2012**, *482*, 547.
26. Agarwal, R.; Jindal, S. K. *Eur. J. Intern. Med.* **2008**, *19*, 227.
27. Verhamme, K. M.; Afonso, A. S.; van Noord, C.; Haag, M. D.; Koudstaal, P. J.; Brusselle, G. G.; Sturkenboom, M. C. *Pulm. Pharmacol. Ther.* **2012**, *25*, 19.
28. Gross, N. J.; Giembycz, M. A.; Rennard, S. I. *COPD* **2010**, *7*, 141.
29. Miravitlles, M.; Anzueto, A. *Int. J. Chron. Obstruct. Pulmon. Dis.* **2009**, *4*, 185.

30. Kiesewetter, D. O.; Silverton, J. V.; Eckelman, W. C. *J. Med. Chem.* **1995**, *38*, 1711.
31. Rzeszotarski, W. J.; Mcpherson, D. W.; Ferkany, J. W.; Kinnier, W. J.; Noronhablob, L.; Kirkienrzeszotarski, A. *J. Med. Chem.* **1988**, *31*, 1463.
32. Guerra, A.; Campillo, N.; Paez, J. A. *Expert Opin. Ther. Pat.* **2006**, *16*, 723.
33. Tanaka, K. I.; Sato, K.; Aoshiba, K.; Azuma, A.; Mizushima, T. *Am. J. Physiol. Lung Cell. Mol. Physiol.* **2012**.
34. Gavalda, A.; Miralpeix, M.; Ramos, I.; Otal, R.; Carreno, C.; Vinals, M.; Domenech, T.; Carcasona, C.; Reyes, B.; Vilella, D.; Gras, J.; Cortijo, J.; Morcillo, E.; Llenas, J.; Ryder, H.; Beleta, J. *J. Pharmacol. Exp. Ther.* **2009**, *331*, 740.
35. Cheng, Y.; Prusoff, W. H. *Biochem. Pharmacol.* **1973**, *22*, 3099.
36. Sali, A.; Blundell, T. L. *J. Mol. Biol.* **1993**, *234*, 779.
37. Fukunishi, Y.; Mikami, Y.; Nakamura, H. *J. Phys. Chem. B* **2003**, *107*, 13201.
38. Jorgensen, W. L.; Chandrasekhar, J.; Madura, J. D.; Impey, R. W.; Klein, M. L. *J. Chem. Phys.* **1983**, *79*, 926.
39. Wang, J. M.; Cieplak, P.; Kollman, P. A. *J. Comput. Chem.* **2000**, *21*, 1049.
40. Wang, J. M.; Wolf, R. M.; Caldwell, J. W.; Kollman, P. A.; Case, D. A. *J. Comput. Chem.* **2004**, *25*, 1157.
41. Berendsen, H. J. C.; Postma, J. P. M.; Vangunsteren, W. F.; Dinola, A.; Haak, J. R. *J. Chem. Phys.* **1984**, *81*, 3684.
42. Fukuda, I.; Kamiya, N.; Yonezawa, Y.; Nakamura, H. *J. Chem. Phys.* **2012**, 137.
43. Asano, T.; Tanaka, K.; Suemasu, S.; Ishihara, T.; Tahara, K.; Suzuki, T.; Suzuki, H.; Fukudo, S.; Mizushima, T. *Biochem. Biophys. Res. Commun.* **2012**, *420*, 444.
44. McLaughlin, B.; Buendia, M. A.; Saborido, T. P.; Palubinsky, A. M.; Stankowski, J. N.; Stanwood, G. D. *PLoS ONE* **2012**, *7*, e36340.

Please cite this article in press as: Yamashita, Y.; et al. *Bioorg. Med. Chem.* (2014), http://dx.doi.org/10.1016/j.bmc.2014.04.029